



# CHORUS

This is the accepted manuscript made available via CHORUS. The article has been published as:

## Feasibility of enhancing the thermoelectric power factor in $\text{GaN}_{\{x\}}\text{As}_{\{1-x\}}$

P. Pichanusakorn, Y. J. Kuang, C. Patel, C. W. Tu, and P. R. Bandaru

Phys. Rev. B **86**, 085314 — Published 20 August 2012

DOI: [10.1103/PhysRevB.86.085314](https://doi.org/10.1103/PhysRevB.86.085314)

# **A study on the feasibility of enhancing the thermoelectric power factor in $\text{GaN}_x\text{As}_{1-x}$**

P. Pichanusakorn<sup>1</sup>, Y. J. Kuang<sup>2</sup>, C. Patel<sup>1</sup>, C. W. Tu<sup>2</sup>, and P. R. Bandaru<sup>1,2</sup>,

<sup>1</sup>Materials Science Program, Department of Mechanical and Aerospace Engineering,

<sup>2</sup>Department of Electrical and Computer Engineering,

University of California, San Diego, La Jolla, CA 92093

## **Abstract**

This study was motivated by the possibility of using N resonant levels interacting with the GaAs conduction band, in  $\text{GaN}_x\text{As}_{1-x}$  ( $0 < x < 2.5\%$ ), to enhance the density of states effective mass ( $m_d$ ) and consequently the thermoelectric power factor ( $S^2\sigma$ ) - where  $S$  is the Seebeck coefficient and  $\sigma$  is the electrical conductivity. However, it was observed that, compared to GaAs, the power factor was reduced in spite of a small increase in the  $m_d$ . The influences of carrier passivation and dopant type, as well as the changes in the carrier scattering mechanism, which degrades the carrier mobility are discussed.

## I. INTRODUCTION

An enhancement of the power factor  $S^2\sigma$ , where  $S$  is the Seebeck coefficient and  $\sigma$  is the electrical conductivity, is of much importance<sup>1</sup> in obtaining higher thermoelectric (TE) efficiency, at a given temperature,  $T$ , as deduced from the figure of merit,  $ZT (= \frac{S^2\sigma}{\kappa}T)$ , especially as the thermal conductivity,  $\kappa$  seems to be reaching theoretical minimum values<sup>2-4</sup>. For materials that can be described through the Boltzmann transport equation (BTE) - which encompasses most of the commonly used TE materials<sup>5</sup>- it was previously shown<sup>6</sup> that an optimal Seebeck coefficient ( $S_{opt}$ ) exists in the range of 130-200  $\mu\text{V/K}$ . Given the narrow range of  $S$ , a much improved power factor can only be obtained through increased  $\sigma (= ne\mu)$ , implying an increased carrier (of charge  $e$ ) concentration,  $n$ , and mobility,  $\mu$ . In semiconductor based thermoelectrics, there is typically a limit<sup>7</sup> to how much the  $n$  could be increased based on solubility limits of the dopant in the host semiconductor. However, in addition to the solubility limit a fundamental understanding of  $n$  could be obtained through examining the expression obtained through the BTE<sup>8</sup>, *i.e.*,

$$n = \frac{1}{2\pi^2} \left( \frac{2k_B T m_d}{\hbar^2} \right)^{3/2} F_{1/2}(\eta) \quad (1)$$

where  $m_d$  is the density of states (DOS) effective mass,  $\eta$  is the reduced Fermi energy ( $= \frac{E_F}{k_B T}$ )

with the Fermi energy,  $E_F$ , reckoned from the conduction band (CB) minimum, and  $F_{j=1/2}(\eta)$  is

the  $j^{\text{th}}$  order Fermi integral, *i.e.*,  $F_j(\eta) = \int_0^\infty \frac{x^j}{e^{(x-\eta)} + 1} dx$ . From the BTE the  $S$  can also be deduced<sup>8</sup>:

$$S = \mp \frac{k_B}{e} \left[ \frac{(r + 5/2)F_{r+3/2}(\eta)}{(r + 3/2)F_{r+1/2}(\eta)} - \eta \right] \quad (2)$$

The above implies the crucial role of the  $\eta$  and the scattering exponent,  $r$  (from the energy dependent relaxation time,  $\tau(E)$  approximation,  $\tau(E) \sim E^r$ ) in modulating the  $S$  and the  $n$ . For example, it can be seen that as  $\eta$  is increased (/decreased), an increase (/decrease) of the  $n$  and a decrease (/increase) of the  $S$  is obtained. Such a contrary relationship implies an optimal value for  $\eta$  for maximal power factor:  $S^2\sigma$ . However, if  $m_d$  is increased while  $\eta$  is held constant, then  $n$  would increase while  $|S|$  remains constant. Alternately, if  $m_d$  is increased while  $n$  is held constant,  $\eta$  would be reduced with an accompanying enhancement of the  $|S|$ . Additionally, reducing  $r$  would also reduce  $|S|$ <sup>9</sup>.

We then hypothesized that a highly mismatched alloy system (HMA) such as N doped GaAs would be a possible system to explore such dependencies and correlations. When a III-V semiconductor, such as GaAs is doped with N to form the alloy  $\text{GaN}_x\text{As}_{1-x}$ , where typically  $0 < x < 0.1$ , the isovalent N impurity substitutes for the Group V element, with a resonant energy level ( $E_N$ ) that is inside the host semiconductor CB. The interaction between  $E_N$  and the CB has the effect of (a) narrowing the host semiconductor band gap ( $E_g$ ) due to lowering of CB edge by 0.12 eV/atomic % N<sup>10</sup>, (b) reducing the  $\mu$  due to change in scattering processes<sup>11</sup>, and (c) increasing  $m_d$ , all of which would considerably effect the electronic properties. Although the reduction in  $\mu$  is undesirable for improving the power factor, it would be interesting to investigate whether the increased  $m_d$  in N-doped GaAs could enhance  $S^2n$  as was previously observed in Tl-doped PbTe.<sup>12</sup> In our investigations, we were inspired by the possibility of using N resonant levels akin to Tl-resonant states interacting with the PbTe valence band (VB), which

significantly increases the  $m_d$ . In this paper, we aim to indicate the modification of the power factor in HMA alloys such as  $\text{GaN}_x\text{As}_{1-x}$ , through measurement and interpretation of the  $S^2n$  and the  $\mu$ . From a fundamental perspective, the role of the scattering mechanism, through a change of the  $r$  and the modulation of the  $m_d$  will be discussed.

In  $\text{GaN}_x\text{As}_{1-x}$  the modification of band structure was initially described as a result of band anti-crossing (BAC) <sup>13, 14</sup> type interactions between the host GaAs CB and  $E_N$ . Such a model postulates a splitting of the CB into an *upper*  $E_+$  and a *lower*  $E_-$  sub-band, where the latter forms the CB minimum. As  $x$  is increased, the BAC model predicts a monotonic decrease of the CB minimum along with a concomitant increase in the  $m_d$  due to a decreased band curvature. Consequently, the DOS, which is proportional to the  $m_d$ , increases particularly close to the  $E_N$ . Alternately, the added N may aggregate and form *cluster* states with localized energy levels, the location of which is dependent on the N configuration within the clusters<sup>15</sup>. In the LCINS (Linear Combination of Isolated Nitrogen resonant States) framework, such cluster states further increase  $m_d$  (in addition to an increase due to  $E_N$ ) when the cluster energy levels are resonant with the  $E_-$  band<sup>16, 17</sup>. For example, when  $x = 0.5$  % a large increase in  $m_d$  from  $0.067 m_o$  ( $m_o$ : free electron mass) to  $0.150 m_o$  was attributed to such cluster state resonances<sup>16</sup>. However, with increasing  $x$ , the influence of the cluster states could reduce and  $m_d$  may be predicted by the BAC model.

There have been a number of experiments that have measured  $m_d$  in  $\text{GaN}_x\text{As}_{1-x}$  and while most show an enhancement of  $m_d$ , there also seemed to be unclear correlations in terms of the influence of doping, as will be discussed next. A very large increase in  $m_d$  up to  $0.19 m_o$  at  $x = 2$  % was observed in undoped  $\text{GaN}_x\text{As}_{1-x}/\text{GaAs}$  quantum wells, measured *via* cyclotron resonance based techniques<sup>18</sup>. On the other hand, a more moderate enhancement was observed in undoped  $\text{GaN}_x\text{As}_{1-x}$  through magneto-photoluminescence measurements<sup>16, 19</sup> with a maximum  $m_d$  of  $\sim$

$0.15m_o$  at  $x = 1.8 \%$ . On the other hand, thermoelectric technique based measurements have instead shown a decrease in  $m_d$  to  $\sim 0.03m_o$  for Se-doped ( $n$  of  $5\text{-}7\cdot 10^{18}/\text{cm}^3$ )  $\text{GaN}_x\text{As}_{1-x}$  at  $x < 0.4 \%$ <sup>20</sup>. However, a recent report recorded an increase in  $m_d$  to  $\sim 0.16m_o$  for Te-doped ( $n$  of  $3\text{-}5\cdot 10^{17}/\text{cm}^3$ )  $\text{GaN}_x\text{As}_{1-x}$  at  $x \sim 1.7 \%$ <sup>21</sup>. Whether such differences were related to the measurement methods or due to the intrinsic material properties are difficult to understand but could yet indicate the specific influence of doping in changing  $n$ . We then seek to investigate Si-doped (*n-type* doping)  $\text{GaN}_x\text{As}_{1-x}$  and compare the experimental results obtained with prior literature. The aim is to understand the modification of the power factor for possible thermoelectric application.

## II. EXPERIMENTAL DETAILS

Samples of  $\text{GaN}_x\text{As}_{1-x}$  with the N composition ( $x$ ) varying in the range of 0 - 2.5 %, were grown on semi-insulating (100) GaAs substrates by gas source-Molecular Beam Epitaxy (GS-MBE). The substrate was initially heated to 580 °C to desorb native oxide under As overpressure, and a 200 nm buffer layer of GaAs was first grown to mitigate surface roughness related issues. The substrate temperature was then lowered to 500 °C during the growth of the electrically active and relevant doped GaAs or  $\text{GaN}_x\text{As}_{1-x}$  layer, using 7N purity elemental Ga and thermally cracked  $\text{As}_2$  (from  $\text{AsH}_3$ ). N was injected using a 13.56-MHz nitrogen radical beam source. During the growth of the active layer, Si was incorporated through thermal evaporation from an effusion cell into the MBE chamber, with a cell temperature:  $T_{Si}$ , in the range of 1100-1270 °C. Generally, the concentration of Si donors, *i.e.*, [Si], would scale with  $T_{Si}$  as:

$$[\text{Si}] \sim \exp\left(\frac{-A}{k_B T_{Si}}\right) \quad (3)$$

where  $A$  is an experimentally determined constant<sup>22</sup>. The  $x$  was maintained to be  $< 2.5\%$  for reducing the possibility of defect formation, due to film-substrate lattice parameter mismatch and it was also seen that growth with  $x < 0.5\%$  was not very reliable. The growth rate for both the buffer and active layers were  $\sim 0.2$  nm/s. The film thickness was monitored *in situ* through RHEED (reflection high energy electron diffraction) based calibrations.

Subsequent to growth, the N composition ( $x$  in atomic %) was determined through the variation of the lattice constant determined by x-ray diffraction. A Vegard's law based interpolation between the lattice constant of GaAs (0.564 nm) and GaN (0.519 nm) was used<sup>23</sup>. Such a measurement may only account for  $N_{As}$  (such a notation indicates substitutional N on an As site) since N aggregates may not contribute to a change in the lattice constant. Through the additional use of SIMS (secondary ion mass spectroscopy) - which measures the *total* N concentration - the N aggregate concentration could be inferred by subtracting the  $N_{As}$  obtained from x-ray diffraction. However, a recent study that used both SIMS and XRD, for the above reason, indicated that N is incorporated mostly as  $N_{As}$  for  $x < 3\%$ <sup>24</sup>, which falls within the range of compositions studied in this work.

The carrier concentration,  $n$ , was measured through determining the resistivity by the well-known van der Pauw (VDP) methodology and through Hall coefficient measurements. Figure 1 shows the arrangement used for the purpose. Ge/Ni/Au were sequentially deposited via electron beam evaporation for electrical contacts<sup>25</sup>. The contacts were annealed at  $450\text{ }^{\circ}\text{C}$  in flowing  $N_2$  for  $\sim 5$  min in a rapid thermal annealing (RTA) chamber. Samples were placed with the active layer facing down on a sacrificial GaAs substrate during the annealing to minimize loss of As through diffusion. The GaAs and  $GaN_xAs_{1-x}$  layers were patterned through plasma

etching (using 10 sccm of  $\text{BCl}_3$  and 5 sccm of Ar, 200 W, 20 mTorr, yielding an etch rate of  $\sim 1$ -2 nm/second). Further processing and experimental details have been elucidated previously<sup>26</sup>.

### III. RESULTS AND DISCUSSION

#### A. Compensation and passivation affects the carrier concentration, $n$ .

The VDP measurements indicated an increase of  $n$  with  $T_{Si}$  at any given  $x$ . However, at a given  $T_{Si}$ , samples with higher  $x$  were seen to have lower  $n$ . The underlying rationale seems to be due to passivation of the Si donors by N and the relevant issues will be discussed later. To maintain the same  $n$  (which was in the range of  $3 \cdot 10^{17}/\text{cm}^3$  to  $1 \cdot 10^{18}/\text{cm}^3$ ) as  $x$  is increased, the  $T_{Si}$  had to be increased to compensate for such passivation. An empirical model was used to predict the required  $T_{Si}$  for MBE growth by assuming that, for samples grown at the same temperature, that  $n$  scales exponentially as  $1/x$ .

The measured  $n$  was plotted as a function of the  $T_{Si}$  (see Figure 2), from which it was observed that  $n$  increases to  $\sim 7 \cdot 10^{18}/\text{cm}^3$  up to a  $T_{Si} \sim 1250$  °C, beyond which there is a decrease. It has been previously been reported<sup>27, 28</sup> that when the concentration of Si donors, *i.e.*,  $[\text{Si}]$ , exceeds  $5 \cdot 10^{18}/\text{cm}^3$ , the role of electron acceptor defects such as  $\text{Si}_{\text{As}}$ , Ga vacancies, and Si clusters rapidly increases as well. Such defects compensate for electrons from the Si donors, which are normally incorporated on Ga sites (*i.e.*, as  $\text{Si}_{\text{Ga}}$ ), leading to a decrease in  $n$ , as was indeed observed at  $T_{Si} > 1250$  °C. In this regard, a compensation ratio,  $\gamma = \frac{N_D + N_A}{n}$  was defined<sup>29</sup> to indicate the ratio of the concentration of fixed ionized centers to the concentration of mobile charges- here  $N_D$  ( $= \text{Si}_{\text{Ga}}$ ) is the concentration of Si incorporated on Ga sites and performing as donors while  $N_A$  ( $= \text{Si}_{\text{As}}$ ) is the acceptor concentration. It was posited<sup>30</sup> that  $\gamma$  depends on relative



availability of Ga and As vacancies and should be independent of [Si]. However, the formation energy of  $\text{Si}_{\text{As}}$  is lowered as [Si] is increased and  $\gamma$  could therefore increase with [Si]<sup>28</sup>. At least one estimate<sup>27</sup> indicates that  $[\text{Si}_{\text{As}}]$  may be as large as 30% of the total [Si] at  $5 \cdot 10^{18}/\text{cm}^3$ , which implies a  $\gamma$  of  $\sim 2.5$ .

From Equation (3), the  $n$  could then be described as a function of  $T_{\text{Si}}$  through:

$$n = \frac{[\text{Si}_{\text{Ga}}] + [\text{Si}_{\text{As}}]}{\gamma} = \frac{[\text{Si}]}{\gamma} = \frac{B}{\gamma} \exp\left(\frac{-A}{k_B T_{\text{Si}}}\right) \quad (4)$$

where,  $B/\gamma = 3.3 \cdot 10^{42}/\text{cm}^3$  and  $A = 7.1$  eV, as determined from the fitting of the  $n - T_{\text{Si}}$  data of GaAs ( $x=0$ ) samples grown at  $T_{\text{Si}} < 1200$  °C, where it is certain that  $\text{Si}_{\text{As}}$  may be the only/main source of acceptor defects. The above equation is shown as solid line in **Figure 2**. In the case of  $\text{GaN}_x\text{As}_{1-x}$ , a further decrease in  $n$  is observed which could be explained invoking Si-N mutual passivation<sup>31-34</sup>, due to Coulombic interaction between the relatively positive  $\text{Si}_{\text{Ga}}$  and the relatively negative  $\text{N}_{\text{As}}$ . Unlike the long-range electron compensation due to  $\text{Si}_{\text{As}}$ , Si and N may only interact and passivate each other if they are nearest neighbors. Such Si-N interactions which may result in  $\text{Si}_{\text{Ga}} - \text{N}_{\text{As}}$  or  $(\text{Si-N})_{\text{As}}$  (where both Si and N share a single As site) complexes, could diminish the Si donor and N concentrations. This would lead to a reduced  $n$  and if there is sufficient Si-N passivation, the band anti-crossing type energy level interactions are reduced, as were observed by the widening of the band gap back to GaAs level<sup>34</sup>

The extent of passivation was understood through the *doping efficiency*,  $\Phi$ , defined as the ratio of  $n$  in the  $\text{GaN}_x\text{As}_{1-x}$  to that in GaAs, both of which are grown at the same  $T_{\text{Si}}$ , *i.e.*,

$$\Phi = \frac{n(x, T_{\text{Si}})}{n(x=0, T_{\text{Si}})} \quad (5)$$

It was previously reported<sup>35</sup> that  $\Phi$  decreases substantially with  $T_{\text{Si}}$ , presumably due to enhanced Si-N interactions. Such a result is to be interpreted considering the relative concentrations of [N]

and [Si]. For instance, at  $x = 0.5 \%$ ,  $[N] \sim 2.2 \cdot 10^{20}/\text{cm}^3$  (given an atomic density of  $4.4 \cdot 10^{22}/\text{cm}^3$  for GaAs), while from Equation 4 and Figure 2, [Si] would be of the order of  $\gamma \cdot 10^{19}/\text{cm}^3$ . As  $\gamma$  is not expected<sup>29</sup> to be greater than  $\sim 10$  - also see Figure 3, the addition of Si would not much impact the doping efficiency, as Si-N passivation demands near neighbor interactions and modulation of the  $\Phi$  implies that the Si be in proximity to the N, which is improbable through MBE based evaporation. Indeed, Si-N passivation in  $\text{GaN}_x\text{As}_{1-x}$  was not observed when Si was introduced *via* ion-implantation; passivation was only evidenced after annealing at  $T > 600 \text{ }^\circ\text{C}$  for  $t = 10 \text{ s}$ , when the diffusion length,  $L_D (= \sqrt{D_{Si}t})$ , with  $D_{Si}$  being the diffusivity of Si in GaAs<sup>36</sup>, was comparable to the average separation, *i.e.*,  $L_N (= \sqrt[3]{[N]})$  between the N atoms<sup>34</sup>.

In this context, the samples in our study were subject to two heating cycles, *i.e.*, (1) during growth where substrate was held at  $500 \text{ }^\circ\text{C}$  for  $\sim 1000 \text{ s}$  of active layer deposition (200 nm at  $0.2 \text{ nm/s}$ ), and (2) during contact annealing at  $450 \text{ }^\circ\text{C}$  for 300 s. Using the previously quoted  $D_{Si}$  value  $L_D$  was calculated to be 0.07 nm, and 0.01 nm for the two steps, respectively. For an  $x \sim 0.5 - 2.5\%$ , the  $L_N$  is approximately in the range of 1.0 - 1.6 nm. Therefore, bulk diffusion should not be sufficient. However, to explain the extensive passivation in our studies and that of others<sup>33</sup> it was necessary to speculate that surface diffusivity of Si adatoms is higher than that of Si diffusivity in the bulk. Additional enhancement of Si surface diffusion may occur through Coulombic attraction. Considering the Debye length ( $\lambda_D$ ) as a metric for charge interactions, and from  $\lambda_D = \sqrt{\frac{\epsilon_o \epsilon_r k_B T}{e^2 n}}$  where  $\epsilon_o$  is the permittivity of free space,  $\epsilon_r$  is the relative static permittivity of GaAs ( $= 13.1$ ),  $n \sim (3-10) \cdot 10^{17}/\text{cm}^3$ , at  $T = 300 \text{ K}$ , a  $\lambda_D$  in the range of 4- 7 nm was calculated. Since  $\lambda_D > L_N$ , it would now be expected that Coulombic forces between N and Si would need to be considered for Si-N passivation.

## B. Decreased carrier mobility, $\mu$ , in $\text{GaN}_x\text{As}_{1-x}$

The  $\mu$  was found to be significantly decreased by the addition of N (*i.e.*, increasing  $x$  in  $\text{GaN}_x\text{As}_{1-x}$ ) - see Figure 3(a). Additionally, N complexes may also be a significant source of scattering<sup>11</sup>. The sharp reduction below  $x = 0.1\%$ , is in accord with previous reports<sup>20</sup> and is indicative of a sudden change in scattering mechanism, while the more gradual decrease above  $x = 0.1\%$ , may be due to an increase of both  $[\text{N}]$  and  $[\text{Si}]$ . However, since  $[\text{N}] \gg [\text{Si}]$ ,  $\mu$  should be largely independent of  $n$  or  $[\text{Si}]$ . The reduction in  $\mu$  then occurs due to (a) an increase in the  $m_d$  as previously considered, through invoking the BAC model, and (b) due to increased *alloy-like* scattering due to the N<sup>37</sup> compared to the native As<sup>38, 39</sup>.

For comparison, we also plot the variation of  $\mu$  with  $n$  for GaAs, superposed on which are the contours of constant  $\gamma$  - obtained using previous calculations<sup>29</sup>. An increase in the  $\gamma$  could indicate a strong onset of compensation through moieties such as  $\text{Si}_{\text{As}}$ , Ga vacancies, Si clusters, *etc.* The observation of increasing  $\gamma$  with  $n$  is in accordance with the data of Figure 2. Generally, a high  $\gamma$  (say,  $\sim 5$ -10) observed for some samples, *e.g.*, S060 and 1057 in Figure 3(b), likely indicates substantial defect formation and may be used as a guide for growth optimization.

## C. Reduction of the Seebeck coefficient, $S$

The Seebeck coefficient ( $S$ ) of  $\text{GaN}_x\text{As}_{1-x}$  was measured as a function of  $x$ , and is shown in Figure 4(a). To verify the accuracy of our measurements, the  $S$  of GaAs was measured as well and compared to literature values as indicated in Figure 4(b). A good fit between the calculation and measurement was found for  $r = 0.26$ , as suggested through previous Nernst coefficient values<sup>20</sup>. Our calculations also considered the increase in  $m_d$  with  $n$  due to GaAs CB non-

parabolicity<sup>40</sup>. The dominant scattering mechanism in GaAs is considered to be polar optical phonon (POP) scattering<sup>39</sup> which cannot be accurately represented by the simple power law of the form  $\tau(E) \sim E^r$ . However, the scattering rate of POP has different constant values above and below 0.05 eV and a characteristic  $r \sim 0$  for the POP processes may be assumed<sup>41</sup>. The lower  $S$  measured for the samples with  $n \sim 3 \cdot 10^{16}/\text{cm}^3$ , in Figure 4(b), may be due to higher impurity concentration as also indicated through the higher  $\gamma$ - see Figure 3(b). If  $n$  is high enough, then the increased impurity concentration could strengthen strongly-screened ionized scattering, which could explain why the  $S$  values for such samples are modeled as closer to  $r=-1/2$ . On the contrary, if  $n$  is low, then weakly-screened Coulomb scattering could be promoted (with  $r=3/2$ ) and  $S$  would also be increased instead (as can also be seen through Equation 2). Other calculations<sup>29</sup> also suggest an increase in  $S$  with the  $\gamma$  presumably due to the latter type of scattering<sup>41</sup>.

For  $\text{GaN}_x\text{As}_{1-x}$  the relationship between  $S$  and  $x$  as in Figure 4(a), is not clear since  $n$  still varies for most samples and  $S$  decreases with increasing  $n$ . To highlight the trend, data points for samples with  $n$  closest to the average value of  $4 \cdot 10^{17}/\text{cm}^3$  are indicated (as black data points) in this figure, from which it was observed that  $S$  seems to have a minimum at  $x \sim 1\%$ . It was generally seen that the  $S$  for  $\text{GaN}_x\text{As}_{1-x}$  was lower than that of GaAs for all the investigated N compositions. However, the variation in  $n$  may affect such a comparison, as the GaAs sample has the lowest  $n \sim 3 \cdot 10^{17}/\text{cm}^3$ . Therefore, the product  $S^2n$  is indicated in Figure 5. A minimum at  $x \sim 1\%$  was again observed. While such a comparison still showed no enhancement of the  $S^2n$  product for  $\text{GaN}_x\text{As}_{1-x}$  over GaAs, the differences are much smaller. If  $n$  were actually equal, then this figure may suggest that the  $S$  of  $\text{GaN}_x\text{As}_{1-x}$  is at most comparable to that of GaAs. The general decrease in  $S^2n$  may be due to a change in scattering mechanism. The addition of N is

responsible for a large decrease in  $\mu$  through a change from POP to alloy scattering. A decrease of  $r$  by 1/2 can reduce  $S$  by approximately 30-50  $\mu\text{V/K}$ <sup>8</sup>. However, there may yet be an enhancement in  $m_d$ .

#### D. Enhancement of the effective mass, $m_d$ , due to N addition

The DOS effective mass ( $m_d$ ) was calculated from the measured  $S$  and  $n$  as follows:

(1) Given a pair of ( $S$ ,  $n$ ),  $\eta$  was first numerically interpolated from Equation 2. While  $r = 0.26$  was assumed for GaAs,  $r = -1/2$  for  $\text{GaN}_x\text{As}_{1-x}$ , as discussed in the previous section.

(2) The  $m_d$  was estimated from  $m_d = \frac{\pi\hbar^2}{k_B T} \left( \frac{2^{1/2} N_o}{N_e} \right)^{2/3}$  where  $N_o = \frac{n_i}{F_{1/2}(\eta)} \left( \frac{\pi}{4} \right)^{1/2}$  and the number of conduction band valleys/degeneracy,  $N_e = 1$ .

Many issues had to be carefully considered for the above estimation, *e.g.*, the temperature during the  $S$  measurement was typically  $\sim 10$  °C higher than that during the  $n$  measurement, due to Joule heating required to provide a temperature difference in the former. In our calculations, the  $T$  in the  $S$  measurement was used, but if a lower  $T$  (as measured during  $n$ ) is used, then  $m_d$  would have increased by  $\sim 3$  %. However, a more significant source of error was the assumption of an appropriate  $r$  value. Figure 6 shows the values of  $m_d$  that were estimated from our measurements in comparison with the values from literature. Where not explicitly stated, we estimated the  $r$  values from prior experimental data<sup>20</sup> and formulae<sup>42</sup>, which indicated that  $r \sim 0.26$  for GaAs, and decreases to  $\sim -0.6$  for  $\text{GaN}_x\text{As}_{1-x}$  (with  $x = 0.4$  %). The transition to a negative  $r$  for  $\text{GaN}_x\text{As}_{1-x}$  is consistent with the earlier discussion, and justifies the use of  $r$  above.

While Dannecker *et al*<sup>21</sup> used  $r = -1/2$  for  $\text{GaN}_x\text{As}_{1-x}$ , an  $r = 3/2$  was chosen by their group for GaAs (which resulted in a lower  $m_d$  for GaAs of  $\sim 0.048 m_e$ , compared to  $\sim 0.072 m_e$  in

our case, despite similar  $S$  and  $n$  as in Figure 3b) on the basis that (weakly-screened) ionized impurity scattering should dominate for doped samples<sup>29</sup>. However, calculations<sup>39</sup> suggest that POP scattering should be more dominant near room temperature, and additionally the compilation of  $S$ - $n$  data for GaAs in Figure 4(b) does support a smaller  $r$  of  $\sim 0.26$ . On the other hand, Young *et al*<sup>10</sup> observed a strong decrease in  $m_d$  attributed to the narrowing of band gap ( $E_g$ ) in accordance with k-p theory<sup>43</sup> where  $m_d$  was estimated through:

$$\frac{m_d}{m_o} = \frac{m_o E_g}{2P^2} \approx \frac{E_g}{20 \text{ eV}} \quad (6)$$

Here  $P^2$  is a matrix element<sup>43</sup> between the electron wavefunctions (similar for most III-V and II-VI semiconductors). The calculated  $m_d$  was then plotted as in Figure 6, where the reduction of  $m_d$  as predicted by the k-p theory was found to be much less than observed by Young *et al*. On the contrary, Dannecker *et al* observed a drastic increase with large fluctuations in  $m_d$  that appear to follow the LCINS model<sup>16</sup>. As the figure shows, at least two characteristic peaks (at  $x \sim 0.4\%$  and  $x \sim 0.5\%$ ) were predicted by the LCINS model and attributed to the contribution from the cluster states of N-Ga-N and N-Ga-N-Ga-N chains<sup>16</sup> respectively. In the absence of effective, interacting cluster states, say at  $x \sim 1\%$ , the  $m_d$  reverts to the BAC model predicted levels.

In the present work, we observe an increase in the  $m_d$  that is more in agreement with the BAC model<sup>13</sup>. However, the observation of a local minimum at  $x \sim 1\%$ , which coincides with both Dannecker *et al*'s results<sup>21</sup> and the LCINS model was puzzling. While the absence of a peak at  $x$  of 0.3%, 0.5%, or 1.7% could be due to the absence of effective N aggregates, a decrease of  $m_d$  below the level predicted by the BAC model is unexpected since  $E_N$  should always be present. It was worth noting that the reduction was close to the level predicted by k-p theory, which may indicate that the band gap reduction could indeed affect the  $m_d$  for  $\text{GaN}_x\text{As}_{1-x}$ .

The absence of contribution from N aggregates may be related to the use of different dopant species in each experiment. While the samples in our study were Si doped, those of Dannecker *et al*<sup>21</sup> and Young *et al*<sup>20</sup> were doped with Te and Se, respectively. While Si may be incorporated into both Ga and As lattice sites, Te and Se would be solely substituting for As. Consequently, amphoteric defect compensation is absent in Te- or Se-doped GaAs. However, Ga vacancy defects still arise as [Te] is increased, which similarly limits  $n$  in GaAs<sup>44</sup>. Furthermore, Te and Se also cannot mutually passivate N, which also only substitutes for As (while Te and Se may be attracted to N through Coulombic forces, they cannot form a direct bond to N as As sites are necessarily separated by Ga sites<sup>44</sup>). It is then possible to deduce, through our experiments, that Si may interact and bond with N aggregates, and is a possible source of large increase in  $m_d$ , as predicted through the LCINS model. While passivation has been described, hitherto, in terms of bonding of single  $\text{Si}_{\text{Ga}}$  to single  $\text{N}_{\text{As}}$ , it is conceivable that Si could also replace Ga in N clusters, *e.g.*, N-Ga-N, as well. The passivation of such aggregates could prevent an increase in  $m_d$ . However, considering that the concentration of such N aggregates could only be a small fraction of the incorporated  $\text{N}^{15}$ , and that since [N] is still much greater than that of [Si], the overall increase in  $m_d$  would be due to BAC like models.

#### IV. CONCLUSIONS

We began with the hypothesis that the interaction between N resonant energy level and the GaAs CB could introduce a large increase in  $m_d$  and consequently enhance the thermoelectric power factor. To test this hypothesis, the  $\sigma$  and  $S$  of Si-doped  $\text{GaN}_x\text{As}_{1-x}$  thin films with  $n$  of  $\sim 3 \cdot 10^{17}/\text{cm}^3$  and  $0.5\% < x < 2.5\%$  were measured. While it was found that  $m_d$  was indeed increased in accordance with the established BAC model, an enhancement in  $S^2n$  compared to

GaAs was not found due to a change in scattering mechanism in  $\text{GaN}_x\text{As}_{1-x}$  which may counteract the increase in  $m_d$  and degrades the  $\mu$  as well. Therefore, one may conclude that the investigated  $\text{GaN}_x\text{As}_{1-x}$  may not be a viable thermoelectric material. However, a comparison of ion implanted Si doped  $\text{GaN}_x\text{As}_{1-x}$  where the effects of Si-N passivation could be reduced, and which should then show an increased  $m_d$  and  $S$  as predicted by the LCINS model, to the results of this work would be necessary to verify such a conclusion. Additionally, other variants where Bi is used instead of N with GaAs (the Bi energy level is now resonant with the GaAs VB<sup>45</sup>) could also be studied for enhanced power factor in that the hole carrier mobility in such materials was shown to be reduced to a much smaller extent<sup>46</sup>.

#### ACKNOWLEDGMENTS

We gratefully acknowledge support from the National Science Foundation (Grant ECS-05-08514)



**REFERENCES**

- 1 P. Pichanusakorn and P. R. Bandaru, J. Appl. Phys. **107**, 074304 (2010).
- 2 M. V. Simkin and G. D. Mahan, Phys. Rev. Lett. **84**, 927 (2000).
- 3 D. G. Cahill, W. K. Ford, K. E. Goodson, G. D. Mahan, A. Majumdar, H. J. Maris, R. Merlin, and S. R. Phillpot, J. Appl. Phys. **93**, 793 (2003).
- 4 D. G. Cahill, S. K. Watson, and R. O. Pohl, Phys. Rev. B: Condens. Matter **46**, 6131 (1992).
- 5 *Thermoelectrics Handbook: Macro to Nano* (CRC Press, Boca Raton, FL, 2006).
- 6 P. Pichanusakorn and P. R. Bandaru, Appl. Phys. Lett. **94**, 223108 (2009).
- 7 W. Walukiewicz, Physica B **302-303**, 123 (2001).
- 8 P. Pichanusakorn and P. R. Bandaru, Materials Science & Engineering, R **67**, 19 (2010).
- 9 P. Pichanusakorn and P. Bandaru, Appl. Phys. Lett. **94**, 223108 (2009).
- 10 U. Katsuhiko, M. Nobuki, and S. Ikuo, Appl. Phys. Lett. **74**, 1254 (1999).
- 11 S. Fahy and E. P. O'Reilly, Physica E: Low-dimensional Systems and Nanostructures **21**, 881 (2004).
- 12 J. P. Heremans, V. Jovovic, E. S. Toberer, A. Saramat, K. Kurosaki, A. Charoenphakdee, S. Yamanaka, and G. J. Snyder, Science **321**, 554 (2008).
- 13 W. Shan, W. Walukiewicz, J. W. Ager, E. E. Haller, J. F. Geisz, D. J. Friedman, J. M. Olson, and S. R. Kurtz, Phys. Rev. Lett. **82**, 1221 (1999).
- 14 T. Mattila, S.-H. Wei, and A. Zunger, Physical Review B **60**, R11245 (1999).
- 15 P. R. C. Kent and A. Zunger, Physical Review B **64**, 115208 (2001).
- 16 F. Masia, et al., Physical Review B **73**, 073201 (2006).
- 17 A. Lindsay and E. P. O'Reilly, Phys. Rev. Lett. **93**, 196402 (2004).

- 18 P. N. Hai, W. M. Chen, I. A. Buyanova, H. P. Xin, and C. W. Tu, *Appl. Phys. Lett.* **77**,  
1843 (2000).
- 19 F. Masia, A. Polimeni, G. Baldassarri, H. von Hogersthal, M. Bissiri, M. Capizzi, P. J.  
Klar, and W. Stolz, *Appl. Phys. Lett.* **82**, 4474 (2003).
- 20 D. L. Young, J. F. Geisz, and T. J. Coutts, *Appl. Phys. Lett.* **82**, 1236 (2003).
- 21 T. Dannecker, Y. Jin, H. Cheng, C. F. Gorman, J. Buckeridge, C. Uher, S. Fahy, C.  
Kurdak, and R. S. Goldman, *Physical Review B* **82**, 125203 (2010).
- 22 T. Tomooka, Y. Shoji, and T. Matsui, *Journal of the Mass Spectrometry Society of Japan*  
**47**, 49 (1999).
- 23 W. G. Bi, F. Deng, S. S. Lau, and C. W. Tu, *J. Vac. Sci. Technol., B* **13**, 754 (1995).
- 24 W. J. Fan, S. F. Yoon, T. K. Ng, S. Z. Wang, W. K. Loke, R. Liu, and A. Wee, *Appl.*  
*Phys. Lett.* **80**, 4136 (2002).
- 25 M. Heiblum, M. I. Nathan, and C. A. Chang, *Solid State Electronics* **25**, 185 (1982).
- 26 P. Pichanusakorn, University of California, 2012.
- 27 S. Schuppler, D. L. Adler, L. N. Pfeiffer, K. W. West, E. E. Chaban, and P. H. Citrin,  
*Appl. Phys. Lett.* **63**, 2357 (1993).
- 28 C. Domke, P. Ebert, M. Heinrich, and K. Urban, *Physical Review B* **54**, 10288 (1996).
- 29 D. L. Rode and S. Knight, *Physical Review B* **3**, 2534 (1971).
- 30 Y. G. Chai, R. Chow, and C. E. C. Wood, *Appl. Phys. Lett.* **39**, 800 (1981).
- 31 J. Li, P. Carrier, S.-H. Wei, S.-S. Li, and J.-B. Xia, *Phys. Rev. Lett.* **96**, 035505 (2006).
- 32 A. Janotti, P. Reunchan, S. Limpijumnong, and C. G. Van de Walle, *Phys. Rev. Lett.* **100**,  
045505 (2008).
- 33 Y. Jin, et al., *Appl. Phys. Lett.* **95**, 092109 (2009).

- <sup>34</sup> K. M. Yu, W. Walukiewicz, J. Wu, D. E. Mars, D. R. Chamberlin, M. A. Scarpulla, O. D. Dubon, and J. F. Geisz, *Nature Materials* **1**, 185 (2002).
- <sup>35</sup> P. Pichanusakorn, Y. J. Kuang, C. J. Patel, C. W. Tu, and P. R. Bandaru, *Appl. Phys. Lett.* **99**, 072114 (2011).
- <sup>36</sup> E. F. Schubert, J. B. Stark, T. H. Chiu, and B. Tell, *Appl. Phys. Lett.* **53**, 293 (1988).
- <sup>37</sup> S. Fahy, A. Lindsay, H. Ouerdane, and E. P. O'Reilly, *Physical Review B* **74**, 035203 (2006).
- <sup>38</sup> M. P. Vaughan and B. K. Ridley, *Physical Review B* **75**, 195205 (2007).
- <sup>39</sup> M. P. Vaughan and B. K. Ridley, in *Dilute III-V Nitride Semiconductors and Material Systems*, edited by A. Erol (Springer-Verlag, Heidelberg, 2008), Vol. 105, p. 255.
- <sup>40</sup> A. Raymond, J. L. Robert, and C. Bernard, *Journal of Physics C: Solid State Physics* **12**, 2289 (1979).
- <sup>41</sup> M. Lundstrom, *Fundamentals of Carrier Transport* (Cambridge University Press, Cambridge, UK, 2000).
- <sup>42</sup> D. L. Young, T. J. Coutts, and V. I. Kaydanov, *Rev. Sci. Instrum.* **71**, 462 (2000).
- <sup>43</sup> P. Yu and M. Cardona, *Fundamentals of Semiconductors: Physics and Material Properties* (Springer, New York, 2005).
- <sup>44</sup> J. Gebauer, E. R. Weber, N. D. Jager, K. Urban, and P. Ebert, *Appl. Phys. Lett.* **82**, 2059 (2003).
- <sup>45</sup> S. Francoeur, M. J. Seong, A. Mascarenhas, S. Tixier, M. Adamczyk, and T. Tiedje, *Appl. Phys. Lett.* **82**, 3874 (2003).
- <sup>46</sup> D. A. Beaton, R. B. Lewis, M. Masnadi-Shirazi, and T. Tiedje, *J. Appl. Phys.* **108**, 083708 (2010).

### Figure Captions

**Figure 1** The layout of the van der Pauw arrangement for the measurement of the thermoelectric power factor ( $S^2\sigma$ ) characteristics of the  $\text{GaN}_x\text{As}_{1-x}$  samples. Four-point measurements of the electrical resistance were carried out for determining the conductivity ( $\sigma$ ) in conjunction with Hall measurements for the mobility ( $\mu$ ) and carrier concentration ( $n$ ). The heating lines/heaters for establishing a temperature gradient for the Seebeck coefficient ( $S$ ) are also indicated.

**Figure 2** The variation of the carrier concentration ( $n$ ) with  $T_{Si}$  (the Si cell temperature in the MBE) for GaAs and  $\text{GaN}_x\text{As}_{1-x}$  samples, indicating the compensation and passivation regimes.

### Figure 3

**(a)** The variation of the carrier mobility ( $\mu$ ) of  $n\text{-GaN}_x\text{As}_{1-x}$  as a function of N composition. The comparison of our data to that of (a) Young *et al* (see Ref. 20) and (b) Skierbiszewski *et al* (see Ref. 47) is indicated.

**(b)** A comparative variation of the carrier mobility ( $\mu$ ) of  $n\text{-GaAs}$  with carrier concentration compared to that of a representative study from literature, *i.e.*, (a) Homm *et al* (see Ref. 48). The dashed lines were adapted from the prior calculations of (b) Rode *et al* (see Ref. 29).

### Figure 4

**(a)** The Seebeck coefficient ( $S$ ) of Si doped  $\text{GaN}_x\text{As}_{1-x}$  as a function of N composition ( $x$ ).

**(b)** The  $S$  vs. carrier concentration ( $n$ ) of  $n\text{-GaAs}$  as measured in this work, and compared to that of (a) Emelyanenko *et al* (see Ref. 49), (b) Homm *et al* (see Ref. 48), (c) Dannecker *et al* (see

Ref. 21), and (d) Young *et al* (see Ref. 20). The analytical calculation assuming various  $r$  values are indicated through lines.

**Figure 5** The variation of  $S^2n$  of Si doped  $\text{GaN}_x\text{As}_{1-x}$  as a function of N composition ( $x$ )

**Figure 6** The density of states effective mass ( $m_d$ ) as a fraction of the bare electron effective mass,  $m_o$ ) comparing three types of dopant, (a) Si,  $n \sim (3-10) \cdot 10^{17}/\text{cm}^3$  as in this work, (b) Te,  $n \sim (3-5) \cdot 10^{17}/\text{cm}^3$  from Dannecker *et al* (see Ref. 21<sup>21</sup>), and (c) Se,  $n \sim (5-7) \cdot 10^{18}/\text{cm}^3$  from Young *et al* (see Ref. 20<sup>20</sup>) Theoretical models were reproduced from earlier work, *e.g.*, (d) LCINS model by Masia *et al* (see Ref. 16), (e) BAC model by Shan *et al* (see Ref. 13) and the (f) k-p model by Katsuhiko *et al* (see Ref. 10). The error bar for our data is small and invisible at this scale, while that for Dannecker *et al*'s data, the error bars ( $= \pm 0.019$ ) were omitted for clarity.

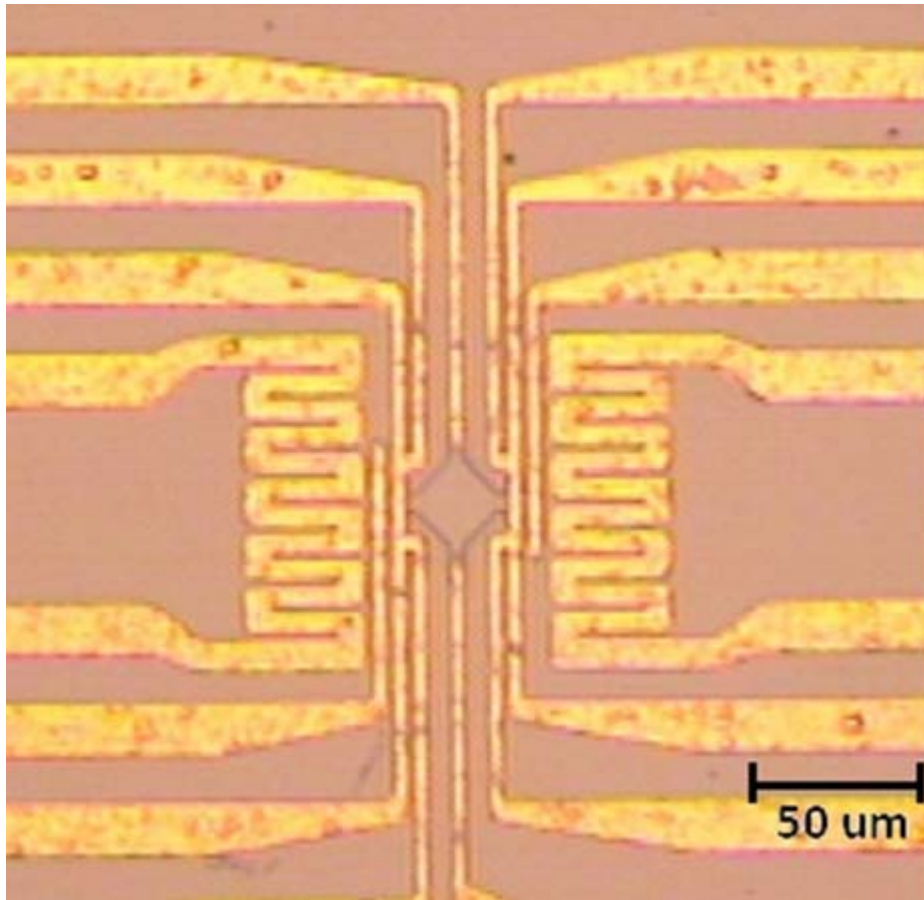
**Figure 1**

Figure 2

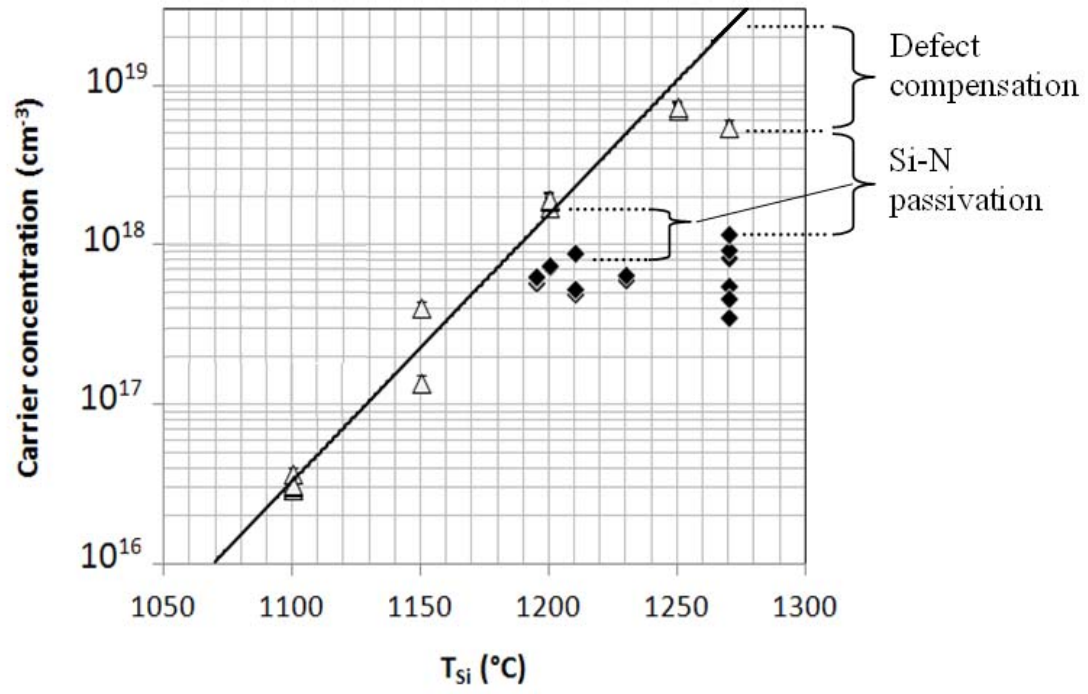


Figure 3

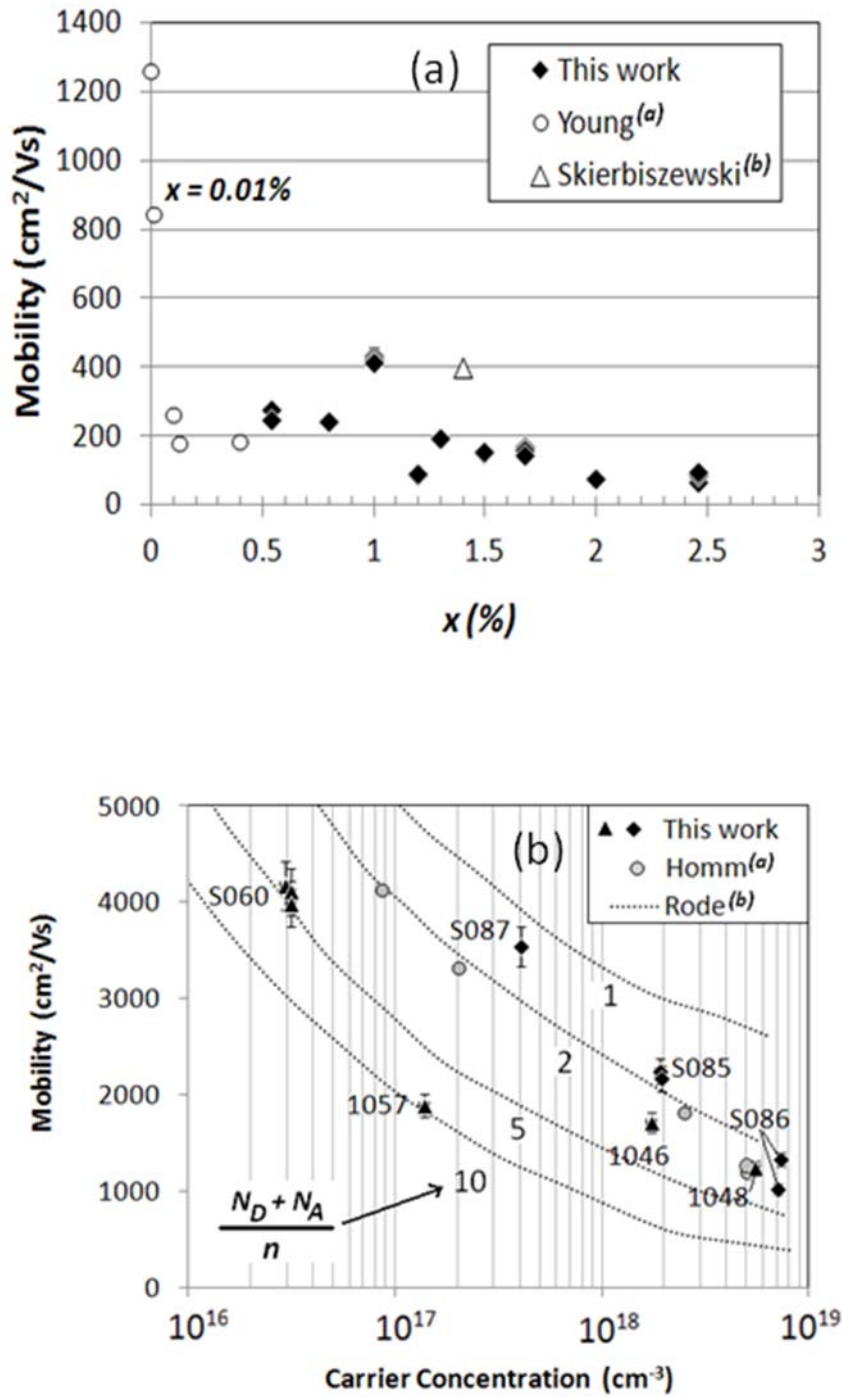




Figure 4

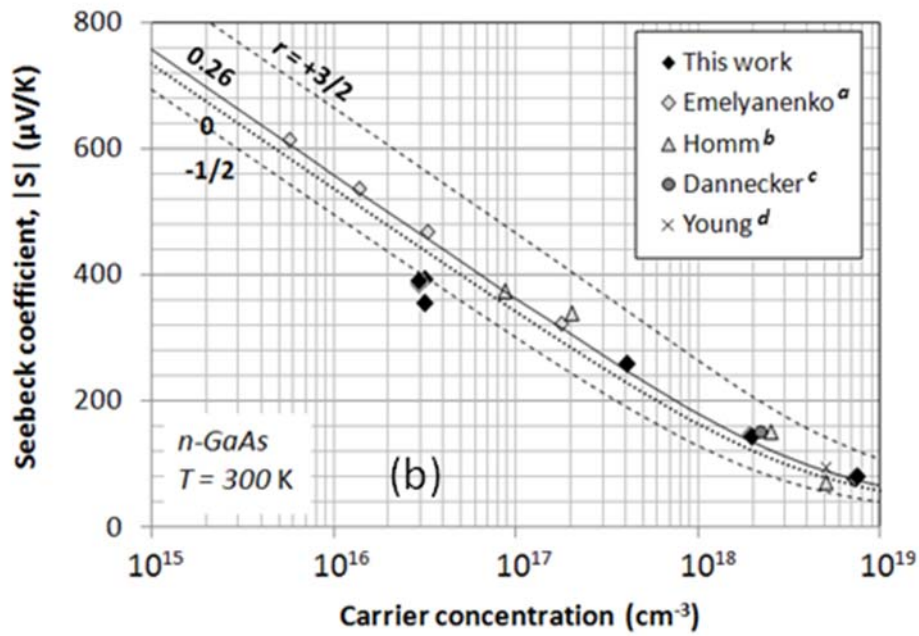
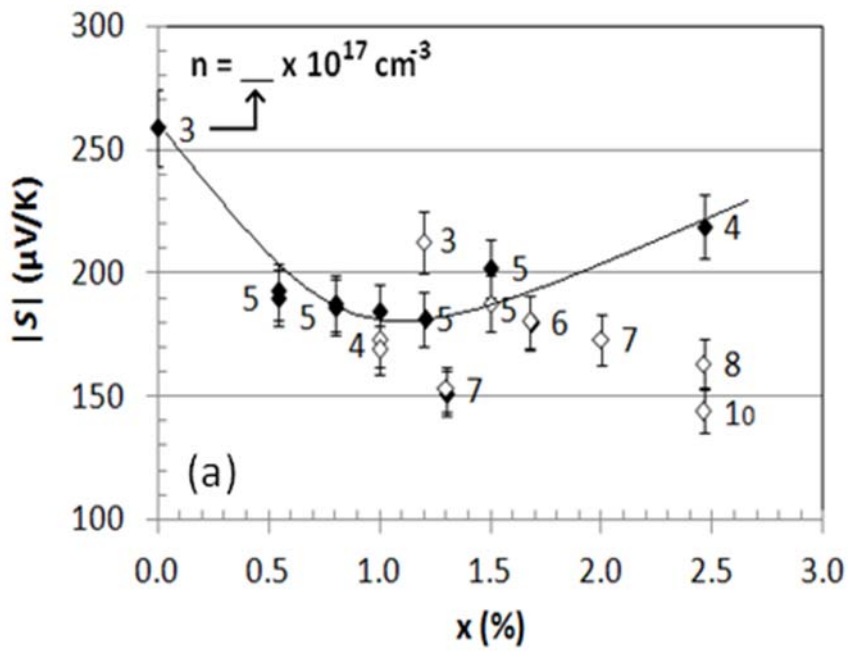


Figure 5

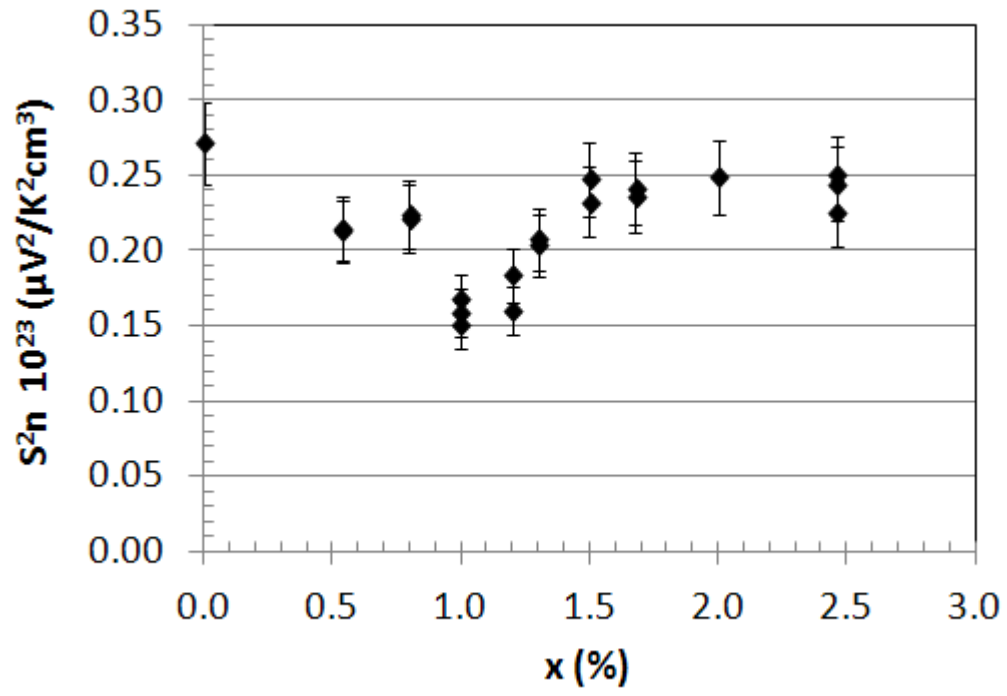


Figure 6

